Comparative Medicine
Copyright 2023
by the American Association for Laboratory Animal Science

Vol 73, No 6
December 2023
Pages 474–485

Original Research

AC-DC Electropenetrography as a Tool to Quantify Probing and Ingestion Behaviors of the Yellow Fever Mosquito (*Aedes aegypti*) on Mice in Biocontainment

Lyndsi D Vaughan,[1,†] Samuel B Jameson,[2,†] Dawn M Wesson,[2] Kristopher S Silver,[3] Dana N Mitzel,[4] Georgina L Dobek,[1] and Berlin Londoño-Renteria[2,*]

A detailed understanding of mosquito probing and ingestion behaviors is crucial in developing novel interventions to interrupt the transmission of important human and veterinary pathogens, but these behaviors are difficult to observe as the mouthparts are inserted into the skin of the host. Electropenetrography (EPG) allows indirect observation, recording, and quantification of probing and ingestion behaviors of arthropods by visualizing the electrical waveform associated with these behaviors. The study of mosquito probing and ingestion behaviors has been limited to the use of human hands as host, which is not suitable for pathogen transmission studies. Mouse models of mosquito-borne diseases are a widely used and indispensable tool in this research, but previous attempts to use direct current EPG to study mosquito probing behaviors on mice have been unsuccessful. Accordingly, the present study used alternating or direct current (AC-DC) EPG to observe the ingestion behaviors of adult *Aedes aegypti* mosquitoes on a mouse host in real time under BSL-2 containment conditions with enhanced BSL-3 practices. Our results show that waveform families previously identified during *Ae. aegypti* probing and ingestion on human hands were observed using 100 mV of AC at an input resistance (Ri) of 10^7 Ohms (Ω) on CD1 mice. This work is a proof of concept for using mouse models for studying mosquito probing and ingestion behaviors with AC-DC EPG. In addition, these data show that the experimental setup used in these experiments is sufficient for conducting studies on mosquito probing and ingestion behaviors under BSL-2 containment conditions enhanced with BSL-3 practices. This work will serve as a foundation for using EPG to investigate the effects of pathogen infection on mosquito probing behaviors and to understand the real-time dynamics of pathogen transmission.

Abbreviations and Acronyms: AC-DC, alternating or direct current; ACL-2EPG, Arthropod Containment Level-2 electropenetrography; DENV, dengue virus

DOI: 10.30802/AALAS-CM-23-000037

Introduction

A detailed understanding of mosquito behavior is crucial in developing novel interventions to interrupt the transmission of important mosquito-borne pathogens. Mosquitoes are among the most important arthropod vectors of pathogens of public health and veterinary importance worldwide. *Aedes* mosquitoes alone put as much as half of the world's human population at risk for contracting one of the many viruses they are known to transmit.[36] The detrimental economic impact of mosquito-borne diseases in communities includes expenditures in vector control programs, education, and restrictions in tourism and trade.[16,30,31] Worse is the enormous morbidity and mortality attributable to mosquito-borne diseases like dengue, Zika, chikungunya, and malaria.[1,36]

To improve our knowledge about the factors involved in transmission and pathogenesis, animal models are traditionally favored in research of mosquito-borne viruses (arboviruses) because in vitro assays are unable to replicate the complex immune system interactions found in natural infections. In this regard, mouse models are the best-characterized mammalian host for these studies with the availability of well-characterized mouse strain models for several arboviruses that allow for in-depth investigation and translation of vaccine and therapeutic applications that are relevant to human health

Dengue virus (DENV) is the most widespread mosquito-borne virus significantly impacting human health.[36] Researchers have found increasing evidence that DENV infection in the primary mosquito vector species, *Aedes aegypti*, causes physiologic and behavioral changes that support the transmission of DENV when the vector takes a blood meal.[25,26,28] DENV infection of *Ae. aegypti* changes the expression of genes related to blood-feeding behavior[33] providing a mechanistic explanation for the

Submitted: 01 Jun 2023. Revision requested: 27 Jul 2023. Accepted: 31 Oct 2023.
[1]Department of Comparative Medicine, Tulane University, New Orleans, Louisiana, [2]Department of Tropical Medicine, Tulane University, New Orleans, Louisiana, [3]Department of Entomology, Kansas State University, Manhattan, Kansas, and [4]National Bio and Agro-Defense Facility, USDA Agricultural Research Service, Manhattan, Kansas
[†]These authors contributed equally to this study
[*]Corresponding author. Email: blondono@tulane.edu

significant changes to host-seeking and blood-feeding behaviors observed in DENV-infected *Ae. aegypti* by high-resolution video capture and analysis.[40] However, current methods are able only to analyze behaviors outside of the host animal, such as attraction and number and duration of feeding events. The knowledge gaps that persist in this field of research are largely caused by the difficulty of assessing the mechanics of mosquito bites and pathogen transmission below the surface of the skin. A better characterization of mosquito bite (that is, probing) events may provide insights that can be exploited to interrupt or decrease the chance of transmission. In the past, the equipment and technology available to observe, record, and interpret the behavior and bite dynamics of mosquitoes have been limited.

EPG is one way to precisely observe the probing and ingestion behaviors of mosquitoes. Early constructs of the EPG were advanced for their time, but great strides have been made in technology since the initial studies.[18,19,21,22,27,35] EPG using alternating or direct current (AC-DC) was first invented in the early 1970s and was used for studying plant-feeding insects and, subsequently, the impact of bacteria transmitted during these feedings.[2,3,38] EPG has developed into a standardized scientific field that utilizes the technology to answer a range of challenging questions from the effects and mechanisms of agriculture pesticides to the egg laying of parasitoid wasps within a host.[5-8] The use of EPG for studying plant-feeding piercing-sucking insects was translated into blood-feeding insects relatively recently with the study of mosquitoes[39] and ticks.[29] Although methods exist to video record mosquito-feeding experiments both outside and, to some degree, within animal tissues,[12,17,40] EPG allows for unique quantification of subsurface behaviors of mosquito mouthparts, especially as it translates to the transmission of pathogens.[2,37,38]

Working with animal models of infectious diseases in the laboratory requires following the standard microbiologic practices for the designated biosafety level.[11] One aim of this study was to test the feasibility of maintaining biocontainment standards suitable for work with risk group 2 pathogens with the intention of conducting future experiments of mosquito-borne virus transmission events in ACL-2 and, eventually, ACL-3 settings. Although no biologic agents were used in this study, the equipment and laboratory space needed to meet institutional and regulatory requirements were used throughout. To our knowledge, this is the first report on the use of AC-DC EPG involving standard laboratory ABSL-2 and Arthropod Containment Level 2 (ACL-2) constraints with enhanced BSL-3 practices in live mice.

Materials and Methods

Mosquitoes. For this experiment, we used blood-naive 10 to 12 d posteclosion, adult female *Ae. aegypti* (Rockefeller strain) mosquitoes. The Rockefeller strain of *Ae. aegypti* has been maintained in laboratories since at least the mid-1930s and is commonly used for laboratory experiments.[23] The mosquitoes were reared following standardized rearing protocols. Briefly, the housing room was maintained at a temperature of 25 to 27 °C, relative humidity 75 to 80%, and a 16:8 light:dark cycle. Mosquitoes were housed in 30 × 30 × 30–cm plastic cages with mesh stockings for entrance holes and given access to a solution of 10% sucrose ad libitum.

For EPG experiments, sucrose solutions were removed from the cage the evening before the EPG recording session to allow approximately 16 h of fasting prior to manipulation. The following morning, 12 to 15 mosquitoes were wired for EPG recordings following previously described methods.[39] Briefly, mosquitoes were cold anesthetized for a maximum of 10 min to minimize side effects of anesthesia. Once anesthetized, mosquitoes were held by gentle suction from a glass tube attached to a vacuum aspirator pump, a small amount of silver glue was applied to the pronotum (Figure 1D), and a gold wire (Figure 1C) was held in the glue until dry. The other end of the gold wire affixed to a brass-plated escutcheon pin (Figure 1A) by a 2- to 3–cm length of copper wire (Figure 1B), deemed an insect stub. Mosquitoes properly tethered to an insect stub were able to fly and walk. Tethered mosquitoes were allowed 3- to 4-h to recover from anesthesia in a small, humid containment box before the EPG recording session.

Animals. Outbred CRL:CD1(ICR) female mice (Strain Code 022, Charles River, Wilmington, MA) $n = 5$; 12 to 18 wk old) were used in this study. Each mouse was used twice with a 2- to 5–d recovery period from anesthesia for $n = 10$ recording sessions. Upon delivery, Charles Rivers verifies that animals are free of the following pathogens: Sendai virus, pneumonia virus of mice, mouse hepatitis virus, minute virus of mice, mouse parvovirus, murine norovirus, Theiler disease virus, reovirus, rotavirus, lymphocytic choriomeningitis virus, ectromelia, mouse adenovirus of mice (types 1 and 2), murine cytomegalovirus, hantavirus, *Bordetella bronchiseptica*, *Citrobacter rodentium*, *Corynebacterium kutscheri*, *Helicobacter* spp., *Klebsiella* spp., *Mycoplasma pulmonis*, *Pasteurella multocida*, *Rodentibacter* spp., *Pseudomonas aeruginosa*, *Salmonella* spp., *Staphylococcus aureus*, *Streptobacillus moniliformis*, *Streptococcus pneumoniae*, β-hemolytic *Streptocuccus* spp., Tyzzer disease, and all ectoparasites and endoparasites.

A housing room was dedicated to the mice used in this short-term study; sentinel testing was not performed. Animals were maintained in an AAALAC-accredited facility in accordance with *The Guide for the Care and Use of Laboratory Animals*.[20] All procedures for animal use were approved by the Tulane University IACUC (Protocol #1484).

Mice were group housed and maintained in static polysulfone autoclavable microisolation mouse cages (186 mmW × 298 mmL × 128 mmH; Allentown, Allentown, NJ) containing hardwood maple bedding (number 7090, Sanichips, Harlan Teklad, Madison, WI; 2 bedding changes weekly) and shredded paper nesting material (Bed-r'Nest, The Andersons, Maumee, OH). Mice were

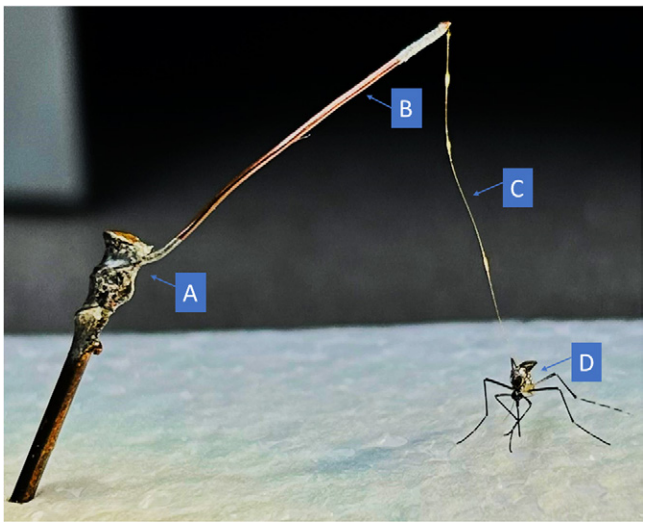

Figure 1. (A) brass-plated escutcheon pin (B) a single strand from a 12-gauge copper wire, 2 to 3 cm in length soldered to escutcheon pin (C) 2 to 3 cm of 0.001 in. gold wire tethering the mosquito to copper wire. (D) Silver glue applied to the pronotum of mosquito.

maintained on a 12:12 light-dark cycle. Temperature (20 to 26 °C; 68 to 79 °F) and humidity (30 to 70%) were maintained with standards outlined in *The Guide for the Care and Use of Laboratory Animals* 8th Edition.[20]

Mice were housed in the Tulane University Department of Comparative Medicine vivarium for at least 2 wk before the start of the study with ad libitum access to acidified water and rodent chow (reference number 5053 Irradiated Laboratory Rodent Diet, Purina, Richmond, IN). Mice were ear tagged and weighed before the start of the experiment.

EPG in biocontainment. An AC/DC EPG system (EPG Technologies Gainesville, FL) and WinDaq software (DATAQ Instruments, Akron, OH) were used to monitor and capture voltage changes during the mosquito blood-feeding process.

The EPG components were arranged to collect readings in a laboratory meeting ABSL-2 and ACL-2 specifications. (Figure 2).

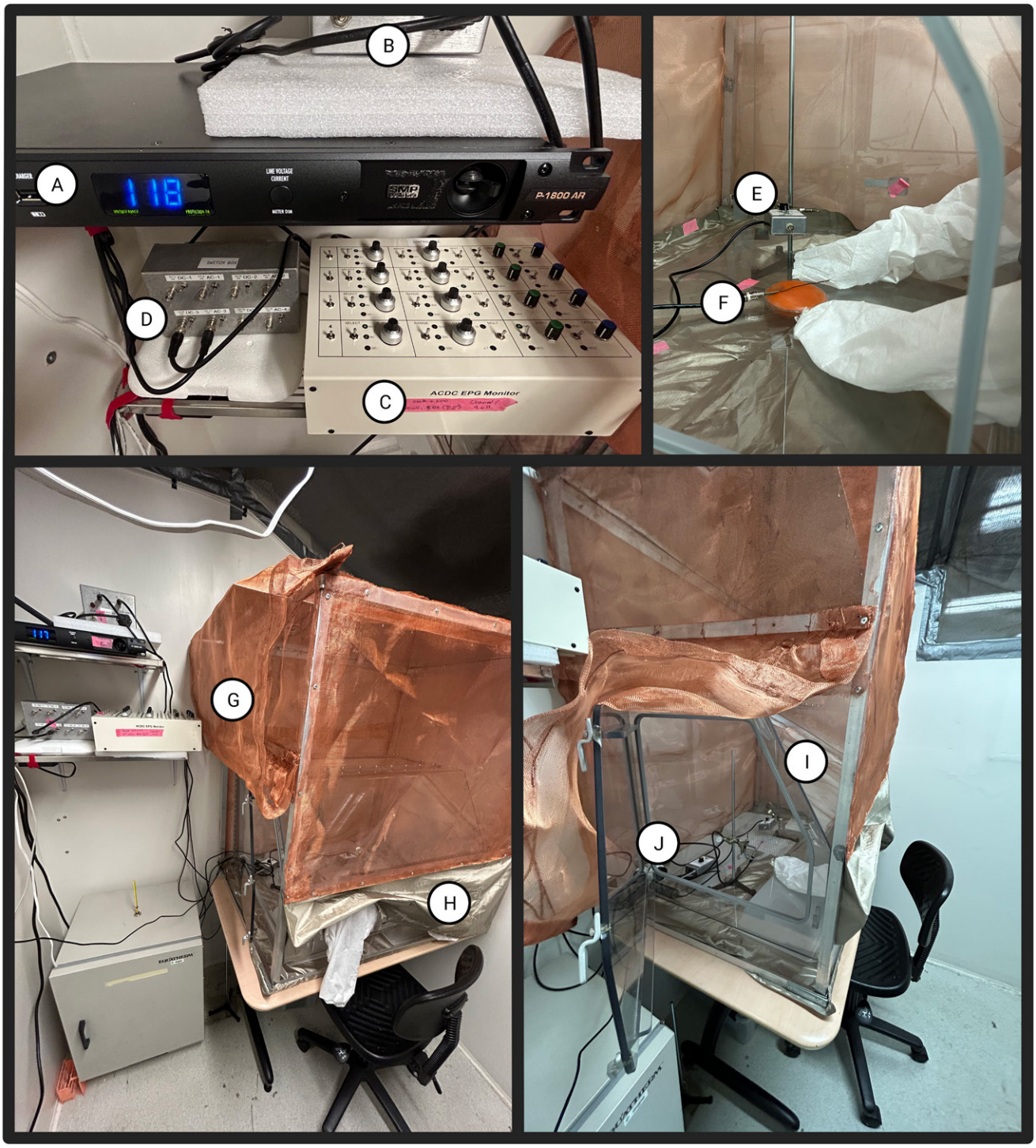

Figure 2. The experimental setup consisted of a (A) Furman P1800 AR power conditioner supplying the (B) EPG power box, (C) AC/DC EPG monitor, and (D) switch box. The head stage amplifier (E) was connected to the switch box while the host probe (F) was connected to the EPG monitor. The workspace was a large Faraday cage with a moveable side panel (G) and front panel (H) that allowed access to and work within a gasketed acrylic glove box (I). All electrical connections within the glove box were passed through a rubber gasketed port (J). The bottom-right panel demonstrates an alternative electrical isolation technique where rubber stoppers are replaced with Nalgene autoclave pans.

The experimental workspace and primary biocontainment apparatus was a gasketed 3′ × 2′ × 2′ acrylic glove box (Coy Laboratory Products, Grass Lake, MI) with a large rubber stopper attached to each bottom corner to electrically isolate the glove box. To reduce ambient electrical noise to the EPG system, the glove box was contained within a custom-built (Dazombie Metals, Metairie, LA) Faraday cage (42″ × 45″ × 30″). The Faraday cage was constructed from 1″ × 1″ solid aluminum right angle and 1″ square aluminum tube stock riveted together with zinc plated right angle braces. A combination of copper screen (16 × 16 mesh, 0.011 diameter wire) and TitanRF Faraday fabric (MOS Equipment, Santa Barbara, CA) was riveted to the outside of 5 sides of the Faraday cage where the bottom side of the cage was left open to sit flush on top of a small fiberboard table. These conductive panels were attached such that each significantly overlapped and was riveted to at least one neighboring panel. The left wall panel and one of the front panels only had one edge secured to the cage to permit access to the interior. The left wall panel was used to add the glove box to the Faraday cage and allowed for loading and unloading of EPG components, animals, and mosquitoes. The front panel was used to access the arm holes of the glove box to manipulate the experimental setup while maintaining biocontainment. The Faraday cage was affixed to the top of its table with screws to prevent accidental movement of the assembly, and a multimeter was used to confirm electrical continuity among the panels before use.

To ground the housing of the head stage amplifier, a tripod cast-iron ring stand was introduced to the workspace through a hole drilled through the floor of the glove box. One of the 3 feet of the stand was sanded to remove the enamel coating and allow for electrical continuity between the head stage amplifier and the Faraday cage. The host probe and head stage amplifier were routed into the glove box through the operable left panel of the Faraday cage and through a foam plugged electrical access port in the rear of the glove box.

Enhanced practices used during this research include the use of class II biosafety cabinets or glove boxes for all mouse manipulations and maintaining, transporting, and manipulating mosquitoes in gasketed locking containers or glove boxes. Secondary arthropod containment was achieved by installing the EPG apparatus within a purpose-built ACL-2 room within an ABSL-2 approved laboratory. The ACL-2 room allowed for controlled access to the experimental area through a self-closing and insect netted doorway and provided a further layer of enhanced practices on top of routine ACL-2 procedures. The ACL-2 room contained the EPG apparatus, a lighted incubator for arthropods, and a second glove box for manipulation of mosquitoes before and after EPG recordings.

Wired mosquitoes were contained in gasketed plastic acclimation boxes to prevent accidental escape by mosquitoes with broken tethers. A spray bottle of 70% isopropyl alcohol and a plastic assay plate covered in adhesive tape were maintained within the experimental glove box to control any mosquitoes breaking free of their tether during EPG recordings.

Experimental outline. Because this was a novel experiment using the EPG equipment on a mouse host, adjustments to the EPG settings were made during individual experiments to optimize the readings. Mice were anesthetized by intraperitoneal injection of a cocktail of ketamine (80 to 150 mg/kg) (Zetamine, VetOne, Boise, ID) and xylazine (5 to 16 mg/kg) (Anased, VetOne, Boise, ID) based on the dose range from laboratory animal–specific formularies for rodents and Tulane institutional care and use committee recommendations on rodent injectable anesthesia cocktails.[15] The fur on both the dorsum and the ventrum of the mouse was shaved to facilitate conduction from the host probe and the mosquito. Artificial tear eye lubricant was placed on both eyes of the mouse to prevent desiccation. The anesthetized mouse was placed in sternal recumbency on the host probe with a reusable small (75 mL) or large (125 mL) sodium acetate heat pad underneath. Each reusable heat pad generated heat from the crystallization of a supersaturated solution of sodium acetate with the total heat produced proportionate to the volume of the sodium acetate solution. After activating a given heat pad, it was massaged and put into use only after the initial spike in temperature had passed and the temperature was judged to be appropriately warm by an ungloved hand. The mouse was placed near the head-stage amplifier for the tethered mosquito to rest comfortably on the dorsum of the mouse (Figure 3).

Before each recording session, the EPG system was turned on and allowed to stabilize for at least 1 h. To perform each recording, the insect stub with attached mosquito was placed into the turned off head stage amplifier such that the flying mosquito was unable to land on the anesthetized mouse and the WinDaq recording was started. The head stage amplifier was then turned on, and a wooden applicator stick was used to bend the copper wire of the insect stub to lower the mosquito onto the dorsum of the mouse. Two to 6 mosquitoes attempted probing on each mouse. All mosquitoes were allowed at least 10 min to attempt probing of the skin to initiate a feeding event. At the completion of the allotted time or if the mosquito was noted to be fully engorged or unlikely to probe again, the mosquito was removed and placed back into a holding container. If the mouse was still at a surgical plane of anesthesia, another mosquito was allowed to attempt probing. One additional dose of ketamine at 50 mg/kg was administered to the mouse intraperitoneally if the mouse was at a light plane of anesthesia, indicated by moving

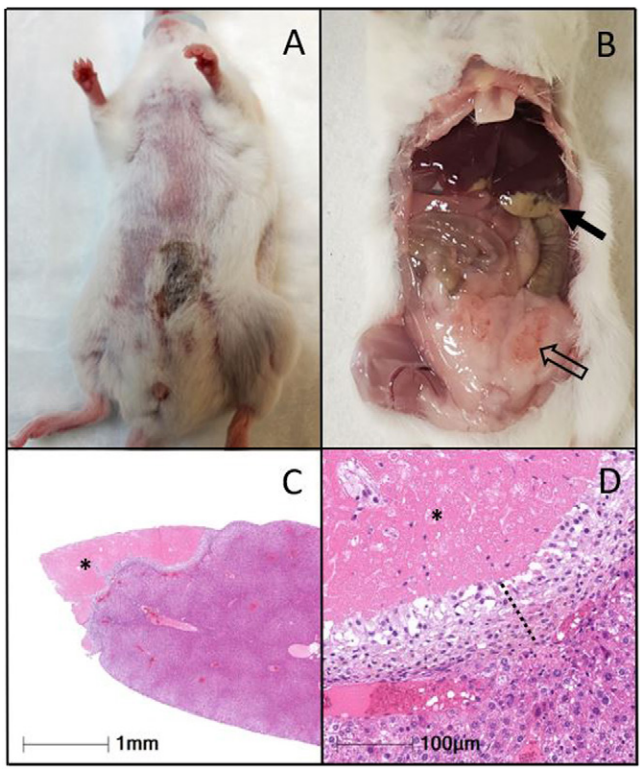

Figure 3. For EPG recordings, anesthetized mice were placed on a copper host probe that was placed on a sodium acetate heating pad. A single mosquito affixed to an insect stub was connected to a head stage amplifier and positioned on the shaved dorsum of the mouse.

or twitching of the limbs, to facilitate multiple recordings. The experiment stopped when the mouse became light under anesthesia after the redose of ketamine or no more wired mosquitoes were available. The mouse was allowed to recover in its home cage with heat support and monitored until fully mobile.

Initial settings of the EPG were at 50 mV AC and 10^7 Ohms (Ω) of resistance. Subsequent readings were with various combinations of voltage, ranging from 50 to 100 mV, and resistance levels were either Ri = 10^7 Ω or Ri = 10^8 Ω. To produce visible and analyzable waveforms, small adjustments of the system gain were made during the initial mosquito feeding event. For this safety and feasibility study, waveform interpretation was limited to the waveform families and types previously outlined for *Ae. aegypti*.[39] Briefly, J refers to low voltage preprobing waveforms that coincide with tapping the proboscis on the epidermal surface and other behaviors before the insertion of the proboscis; K denotes waveforms during the initial penetration of the skin by the mosquito's mouthparts; L1 and L2 are regular and irregular signals, respectively, at a moderate voltage that are currently thought to be generated when the mosquito mouthparts are within the tissue but have not penetrated a blood vessel; M1 and M2 refer to regular and irregular high-voltage signals, respectively, generated during ingestion; N denotes irregular waveforms postingestion that have yet to be linked to a behavior.

Statistical analysis. Waveforms were evaluated in WinDaq software, and the boundaries of each waveform were determined following previously published conventions for *Ae. aegypti*.[39] Waveform labels and durations were calculated by the "FileManipW2 082117" SAS program and checked for errors with the "Error Checker 100716" SAS program Statistics were calculated from the resulting data file using the "Ebert Generic" SAS program to analyze sequential EPG data (all programs are available from https://crec.ifas.ufl.edu/extension/epg/). The Ebert program uses the glimmix procedure to perform ANOVA and calculate least-squares means and errors for multiple outputs of interest. The generic version of the Ebert program can calculate 14 predefined variables, seven of which were identified as appropriate for this study and selected for analysis (Table 1). Waveform K was used to define the beginning of each probe. The default Gaussian distribution was used for all variables except for NumPrbsAftrFrstXY, which used the γ distribution. Underlying assumptions and appropriateness of the models were checked with residual plots and χ^2 goodness-of-fit statistics. Poorly fitting data were log-transformed for final analysis. All analysis steps were performed using SAS software, version 9.4 of the SAS System for Windows.

Results

Impact on mouse host. Initially, the mice were injected intraperitoneally with a cocktail mixture of ketamine at 90.9 mg/kg and xylazine at 9.2 mg/kg. This dose was insufficient on the first mouse with the mouse unable to reach a surgical plane of anesthesia long enough for a probing attempt. Because of the sensitive nature of the EPG equipment, we concluded the mouse's twitching movement would interfere with the recordings and make it difficult to interpret waveforms.

On subsequent mice, we used a cocktail of ketamine at 87.5 mg/kg and xylazine at 12.5 mg/kg. This provided approximately 20 to 25 min of surgical plane anesthesia sufficient to record waveforms without interference from movements of the mouse. To extend the duration of the anesthesia to gather more data points, we redosed the ketamine at 50 mg/kg if the mouse was at a light plane of anesthesia and began moving. This cocktail with redose of ketamine provided approximately 50 to 60 min of surgical plane anesthesia sufficient for recordings for 6 out of 9 sessions. Two of the mice had a prolonged anesthesia time (45 to 60 min) with the ketamine/xylazine cocktail alone and did not receive the redose of ketamine. Consequently, neither mouse recovered from the anesthetic event. Anecdotally, there were fewer probes and no mosquitoes fed to repletion on these 2 mice. One mouse remained at a surgical plane of anesthesia after the initial ketamine/xylazine dose for approximately 25 min but was too light (noted by twitching of limbs, tail, and whiskers) even after the ketamine redose to continue recording. Though this recording session was short, one mosquito fed to repletion and resulted in a full waveform recording.

Animals undergoing anesthesia longer than 10 min were required to have a heat source present for thermoregulation. To reduce electrical interference and facilitate biocontainment, we chose to use reusable sodium acetate heating pads. The copper-wire host probe was placed directly on top of this heat source with the mouse placed on top of the probe. One mouse was noted to have a 1.5 × 1–cm hyperkeratotic lesion (Figure 4A) on the lower left to mid quadrant of the ventrum. At the end of the study,

Table 1. Variables calculated by the Ebert Generic SAS program

Variable name	Description	Inclusion
CtoFrstXY	The number of complete probes before the first XY event	Not included
NumXY	The number of XY events	Not included
DurNnprbBfrFrstXY	The duration of the nonprobe period before the first XY	Not included
NumShrtPrbAftrFrstXY	The number of short probes (<180 s) after the first XY event	Not included
NumLngXY	The number of long (≥600 s) XY events	Not included
TmFrstSusXYFrstPrb	The time it takes to get to the first sustained XY from the start of the first probe	Not included
PrcntProbXY	The percentage of time spent in XY event given the total probing activities time	Not included
TtlDurXY	The total duration of XY for each insect	Included
MeanXY	The mean duration of XY for each insect	Included
MeanNXYPrb	The mean number of XY events per probe by insect	Included
TmFrmFrstPrbFrstXY	The time from the beginning of the first probe to the first XY	Included
TmBegPrbFrstXY	The time from the beginning of the probe with the first XY event to the first XY event	Included
NumPrbsAftrFrstXY	The number of probes after the first XY event	Included
MaxXY	The longest duration of an XY event for each insect	Included

All variables are calculated by insect for a designated waveform type ("XY").

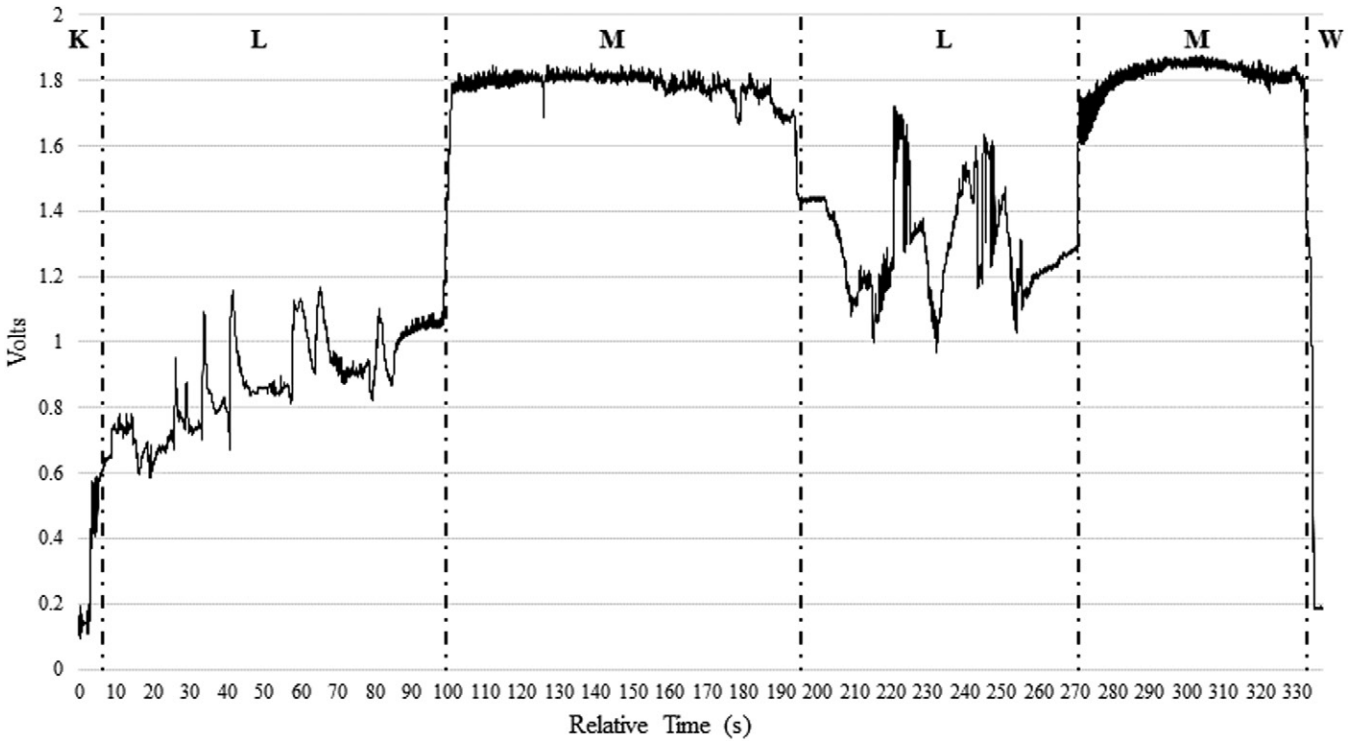

Figure 4. (A) Mouse with a 1.5 × 1–cm hyperkeratotic lesion on the bottom left to mid quadrant of the ventrum. (B) Focally extensive hepatic necrosis on 2 liver lobes (black arrow) with petechial hemorrhage on the caudal fat pad (open arrow). (C) Histopathology of the liver with hematoxylin and eosin stain. There is a sharply demarcated region of coagulative necrosis (asterisks) extending from the margin of the liver lobe. (D) The area of necrosis (asterisks) is separated from viable liver by a band of macrophages (dashed line).

this mouse was euthanized, and a necropsy was performed. Focally extensive hepatic necrosis was noted (Figure 4B). All other organs were within the normal limits grossly. Liver and skin tissues of and around the hyperkeratotic lesion were submitted for histopathology review. Tissues were fixed in 10% formalin buffer, mounted in paraffin, sliced, and stained with hematoxylin and eosin stain. The microscopic findings in this case (Figure 4C and 4D) indicated either thermal or ischemic necrosis of the skin and liver, with the former being most likely given the history.

Waveforms. After system optimization, there were 17 recorded feeding events that were sufficient for analysis across 2 tested treatment levels, Ri = 10^8 Ω (n = 9) and Ri = 10^7 Ω (n = 8). Recorded waveform events were categorized into their respective family based on the appearance of the waveforms compared with the published waveform library for *Ae. aegypti*[39] (Figure 5). Recorded waveforms followed the previously reported feeding pattern for this species and produced characteristic waveforms in each of the waveform families. No observations in this study contradict the previously hypothesized associations of the L and M families with tissue navigation and ingestion, respectively. The optimal settings for EPG recordings on mice were determined to be 100 mV of AC with Ri =10^7 Ω. Although Ri levels of 10^7 Ω and 10^8 Ω provided interpretable waveforms,10^7 Ω produced clearer waveforms during much of L and M (Figures 6 and 7). Recordings at 50 and 75 mV, in general, produced waves with smaller amplitudes that made them more difficult to interpret. Recordings at 10^8 Ω had poor resolution during K and, at higher voltages, produced spiked and noisy signals that complicate interpretation.

Sequential EPG analysis with the Ebert Generic program indicated that there were significant statistical differences between the Ri treatment levels with respect to the 2 waveform families of interest, L and M (Table 2). Of the 4 waveform types assessed, only M1 had no statistical difference between Ri treatment levels across the 7 variables of interest. Waveform L1 was found to differ significantly between Ri treatment levels in total duration (P = 0.0019), longest duration (P < 0.0001), time from beginning of probe to first occurrence (P < 0.0001), time from beginning of probe with first occurrence to first occurrence (P < 0.0001), and number of probes after the first occurrence (P < 0.0001). L2, however, only differed in the number of probes after the first occurrence of L2 (P < 0.0001). M2 waveform types were found to differ significantly between treatments by total duration (P = 0.0117), mean duration (P = 0.0001), longest duration (P = 0.0001), and the number of probes after the first occurrence of M2 (P < 0.0001).

Discussion

We found that biocontainment and biosafety needs can be maintained during EPG recordings of mosquito feedings on mice. Mouse physiology appeared to be compatible with AC-DC EPG recording systems, and observed waveform families from feeding events were identifiable in the published waveform library of *Ae. aegypti*.

Anesthesia and impacts on mice. Finding an anesthetic cocktail suitable for the described setup proved challenging given the number of unknown factors present at the initiation of study. A critical component to evaluating EPG recordings is the accurate interpretation of the waveforms. This means any movement from the mouse that might cause artifactual distortion of the electrical signal or interrupt feeding needed to be minimized without compromising or interfering with normal mosquito probing behaviors. Inhalant anesthetics were considered since they are relatively safe and have a rapid onset and recovery.[15] However, this route of anesthesia was dismissed because of possible exposure of the anesthetic to the mosquito, the constraints of fitting

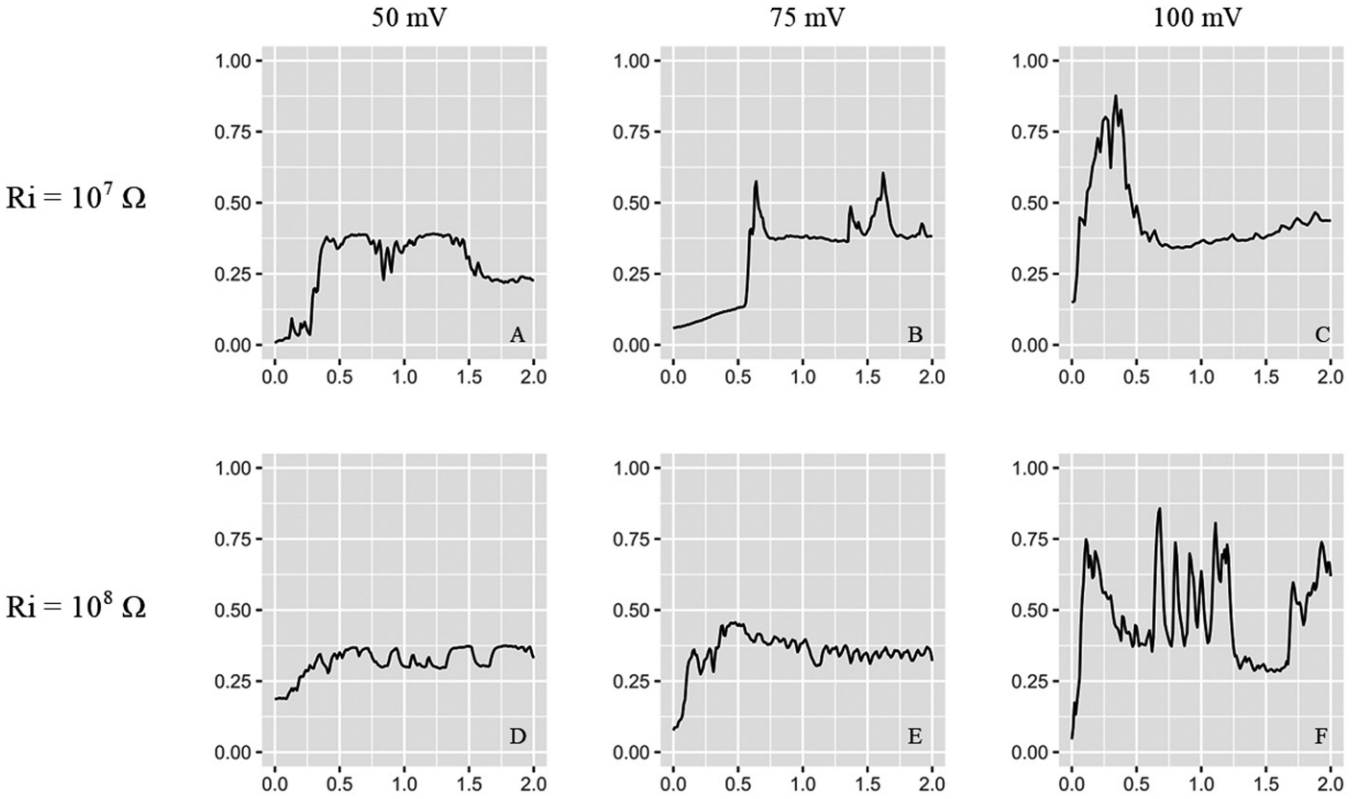

Figure 5. Representative EPG recording (Ri = 10^8 Ω) of *Ae. aegypti* feeding on a mouse in the experimental setup. Raw data were exported and plotted in Microsoft Excel. (K) Waveform K – initial penetration, (L) Waveform L – indeterminant preingestion phase, (M) waveform M–ingestion, (L) waveform L, (M) waveform M, (W) withdrawal of mouthparts.

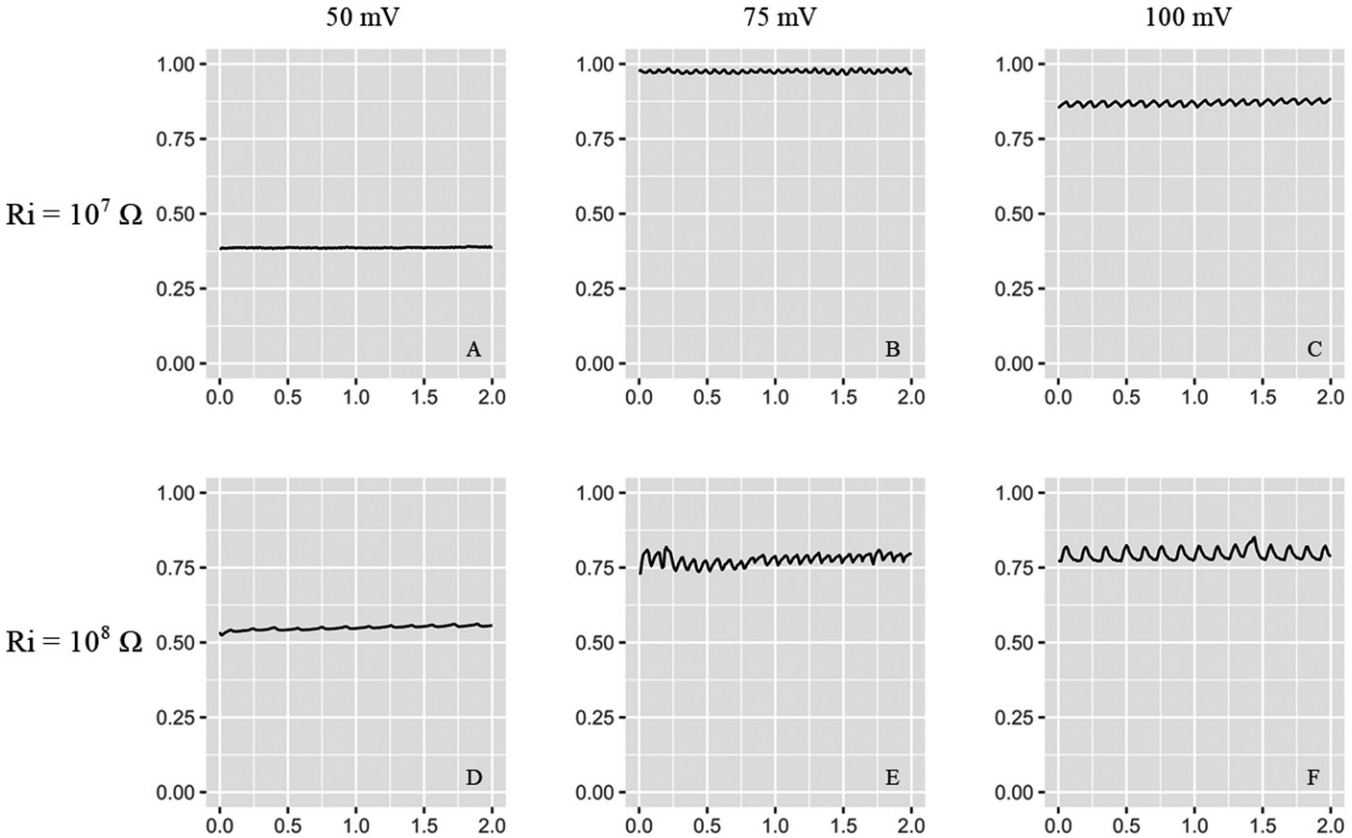

Figure 6. Comparison of representative 2-s normalized samples of K (A–F) at various voltages and Ri levels. In each panel, the *y* axis reflects the normalized voltage and the *x* axis reflects the relative time from zero to 2 s.

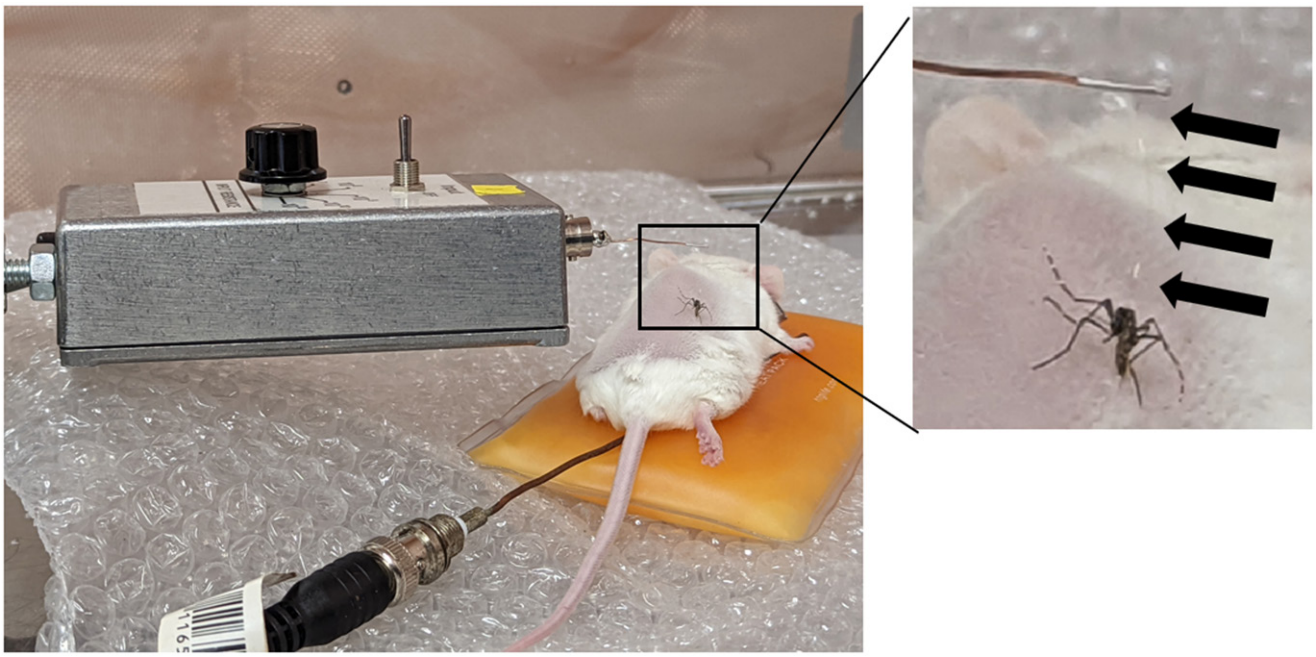

Figure 7. Comparison of representative 2-s normalized samples of M1 (A–F) at various voltages and Ri levels. In each panel, the *y* axis reflects the normalized voltage and the *x* axis reflects the relative time from zero to 2 s.

hoses into a small biocontainment box, and the unknown noise or vibration that could be generated and detected by the EPG instrument. Thus, injectable anesthetic cocktails were chosen for this study. The drug cocktails used to anesthetize the mice were adequate to determine the optimal settings for EPG recordings. However, we determined that, because of the variable and relatively short duration of the chosen cocktails, these mixtures would be inadequate for use in studies with infectious agents in an EPG setting. Although the maximum exposure time for a mosquito to a mouse in our experiments was 10 min, the logistics of inducing anesthesia and shaving the mouse in an appropriate biologic safety cabinet and safely moving it into the glove box within the Faraday cage provides multiple opportunities for delays in initiating the recording. A reliable 30-min plane of anesthesia with immobility would provide enough time to complete a full EPG recording without having to open the primary biocontainment midprocedure to provide additional anesthetic. The anesthetic deaths experienced with the ketamine-xylazine cocktail indicates a need for future EPG studies to consider combining ketamine and xylazine with a phenothiazine derivative, such as acepromazine to provide a more reliable and safer plane of anesthesia.[10,24] The results of the histopathologic findings from the single mouse with necrotizing skin and liver lesions are likely because of burns caused by the copper probe becoming overheated by the larger 125-mL heat pack and being in direct contact with the sensitive shaved skin of the abdomen of the mouse. The smaller 75-mL heat packs were used for all mice after this injury was noted and no further heat injuries were observed. To maintain electrical conductivity for the EPG recordings, the abdominal fur must be removed. In addition, electrically powered warming methods cannot be used because of the delicate electrical environment. Future studies should use the smallest volume chemical heater sufficient for the animal and duration and should employ a thermal break like bubble wrap or paper towels between chemical heaters and the copper host probe. For increased control of heat in this setting, circulating water baths or other similar equipment that allows for the electrical components to remain outside of the Faraday cage may be useful.

For this experiment, we used $n = 5$ mice but used each mouse 2 to 3 times over the course of testing. The EPG recording sessions consisted of a benign procedure which included anesthesia and the bites from mosquitos. We wanted to reduce the number of animals used in the study and reuse them with a minimum of a 48-h rest period before using the same mouse for another EPG recording session. There were no gross sequelae from the mosquito bites on the dorsal skin. This could be explored further in future EPG studies.

EPG results. One aim of this study was to determine whether EPG recordings of *Ae. aegypti* feeding on mice were consistent with published waveforms from *Ae. aegypti* feeding on human hands. Waveforms produced in this EPG and mouse host system were readily identifiable in the published *Ae. aegypti* waveform library from feeding events on human hands.[39] Previous studies that attempted to collect EPG-type data from mosquitoes feeding on mice were only marginally successful because the mosquitoes were not directly wired to the system.[21,22] AC EPG was used exclusively in these studies to avoid potential negative impacts on feeding that have been observed in larger insects with DC EPG.[4,5] We successfully visualized waveforms putatively associated with mosquitoes entering the skin (waveform family J), probing and finding a blood vessel (waveform families K and L), and ingesting blood (waveform family M). We also observed the waveforms from the family N, which currently has an unknown biologic correlation. Waveform families J and N were not observable in all recordings and were omitted from the analysis. When these waveform families were observed they were always immediately because proboscis insertion (family J) or at the very end of a probe (family N). As such, the omission of these waveform families did not negatively impact the sequential data analysis in Ebert. A detailed comparison of EPG waveforms generated from *Ae. aegypti* feeding on mice to published waveforms was not possible given the limited sample size in the present proof of concept study.

Variables omitted from the analysis were NumXY, NumLngXY, PrcntPrbXY, DurNnprbBfrFrstXY, CtoFrstXY, NmbrShrtPrbAftrFrstXY, and TmFrstSusXYFrstPrb. These variables

Table 2. Selected sequential variables calculated from Ebert Generic SAS program

Variable	Ri = 10^7		Ri = 10^8				
	Estimate	SE	Estimate	SE	Num DF	Den DF	Pr > F
L1							
Mean number of L1 occurrences per probe by insect	2.6923	0.2488	2.8750	0.2837	1	44	0.6306
Total duration of L1 for each insect	62.3050	8.7308	18.5055	9.9546	1	44	0.0019†
Mean duration of L1 for each insect	11.4604	1.3173	8.0355	1.5019	1	44	0.0935
Longest duration L1 for each insect	34.3392	1.9778	12.9800	2.2550	1	44	<0.0001†
Time from first probe to first L1*	1.0425	0.2297	2.5917	0.2618	1	44	<0.0001†
Time from beginning of probe containing first L1 to first L1*	1.0425	0.1812	2.2394	0.2065	1	44	<0.0001†
Number of probes after the first occurrence of L1	1.6094	0.0327	0.1542	0.0566	1	22	<0.0001†
L2							
Mean number of L2 occurrences per probe by insect	3.4190	0.2622	3.1465	0.2700	1	66	0.4715
Total duration of L2 for each insect*	4.4827	0.2329	3.8549	0.2398	1	66	0.0648
Mean duration of L2 for each insect*	2.7384	0.1082	2.9717	0.1114	1	66	0.1377
Longest duration L2 for each insect*	4.1336	0.1658	3.7122	0.1708	1	66	0.0813
Time from first probe to first L2*	1.5660	0.0968	1.7317	0.0997	1	66	0.2376
Time from beginning of probe containing first L2 to first L2*	1.5660	0.0968	1.7317	0.0997	1	66	0.2376
Number of probes after the first occurrence of L2	1.6094	0.0347	0.5947	0.0406	1	36	<0.0001†
M1							
Mean number of M1 occurrences per probe by insect	2.4506	0.2318	2.1533	0.2409	1	50	0.3781
Total duration of M1 for each insect*	3.3282	0.2085	3.5201	0.2166	1	50	0.5262
Mean duration of M1 for each insect*	3.0255	0.1056	3.0619	0.1097	1	50	0.8118
Longest duration M1 for each insect	44.870	5.2277	44.8196	5.4327	1	50	0.9947
Time from first probe to first M1*	4.7275	0.2226	4.4506	0.2314	1	50	0.3925
Time from beginning of probe containing first M1 to first M1*	3.9834	0.1308	3.8693	0.1360	1	50	0.5481
Number of probes after the first occurrence of M1	NC	NC	NC	NC	NC	NC	NC
M2							
Mean number of M2 occurrences per probe by insect	2.0333	0.2076	2.3389	0.1695	1	48	0.2600
Total duration of M2 for each insect	26.7185	7.2589	51.27	5.9269	1	48	0.0117†
Mean duration of M2 for each insect	11.1070	1.8287	20.8410	1.4931	1	48	0.0001†
Longest duration M2 for each insect	18.9005	4.8440	44.9703	3.9551	1	48	0.0001†
Time from first probe to first M2*	4.7372	0.2373	4.6908	0.1938	1	48	0.8803
Time from beginning of probe containing first M2 to first M2*	4.0405	0.1697	3.9597	0.1386	1	48	0.7139
Number of probes after the first occurrence of M2	0.6931	0.00002	4.9×10^{-9}	0.00003	1	10	<0.0001†

NC, no change.
*Variables log-transformed to meet assumptions of the statistical program.
†Statistically significance values ($P \leq 0.05$).

were omitted because they are not meaningful in the context of mosquito probing and ingestion behaviors. Although the definitions of long and short probes can be edited within the program, there is not currently enough accumulated EPG data from *Ae. aegypti* to determine where these boundaries might be drawn. The CtoFrstXY variable may prove useful when examining the M family of waveforms in future mosquito studies with experimental conditions that lead to multiple probes prior to successful blood ingestion.

Statistical differences in at least one calculated variable were found between the Ri levels for 3 of the 4 waveform types assessed. At 10^7 Ω, L1 occurred more quickly after K and more time was spent in L1 than at 10^8 Ω. Because L1 and L2 are differentiated by the regularity of the waveform, noisier and sharper signals recorded at 10^8 Ω led to L1 waveform types classified as L2 are possible. Such misclassification would explain all the statically identified duration-based differences between the treatment groups for L1. In the case of misclassification, how this would change the analysis of the L2 waveform type is unclear. Alternatively, this difference could suggest that L1 is dominated by R components that are more readily identifiable at the lower 10^7 Ω Ri level than 10^8 Ω where increased emf components may be detected.

At 10^8 Ω, *Ae. aegypti* were found to spend nearly twice as long in M2 (both total duration and mean duration) than in recordings at 10^7 Ω. The potential for misclassification in the M waveform family is less likely given the clear, high-voltage sinusoidal M1 waveform. The precision of the M1 definition is supported by similar estimates and lack of statistical differences between treatments observed in M1. The differences between the treatment groups with respect to M2 are likely the result of a small sample size. Determining true differences between treatment groups with EPG data is difficult because of the variable nature of insect probing and ingestion behaviors. Although some small sample sizes will, by chance, have excellent uniformity, overdispersed data, distributions with gaps, and zero-inflated data are far more common. As a result, EPG studies seeking to definitively determine differences between treatment groups with the Ebert program have denominator degrees of freedom between 250 and 300.[13,14]

The limited sample size likely also resulted in the difference between the treatment groups in L1, L2, and M2 with respect to the number of probes after the first occurrence of the waveform type. In all cases, *Ae. aegypti* in the 10^7 Ω group were found to be more likely to probe again after the analyzed waveform type. In M1, the sample size was too small and the data were too sparse for the model to converge. As any Ri level change should not be felt by the mosquito, it would be unexpected for an Ri level change to impact this metric. A larger sample size is likely to remove this observed difference. Of note is that the estimates for this variable confirm that a given mosquito is likely to withdraw their proboscis and probe again following L1 or L2 but unlikely to do so after entering M2.

To our knowledge, this is the first report on the use of the Ebert Generic program for mosquito EPG data analysis. Although the program is intended to be useful for EPG data from any arthropod EPG system, the program required editing to operate with conventions used in mosquito EPG data analysis. Future studies should stringently identify waveform family J during initial data coding to allow the program to analyze waveform family K as well. In the present study, K was used to define the beginning of each probe and is, consequently, omitted from analysis.

A limitation of the current study is the small sample size. Currently, no guidelines for estimating samples size for EPG experiments with mosquitoes or on animal hosts have been published. For this reason, this study was kept small to use the fewest number of animals while providing enough data to demonstrate the utility of the AC EPG monitoring of *Ae. aegypti* bites in a mouse model. The inherent variability in feeding times between insects may lead to unreliable statistical estimates with small sample sizes. Sample sizes used for definitive between group determinations with the Ebert program use sample sizes at least 6-fold larger than the current study.[14,32] The optimal settings for this system were determined to be 100 mV of AC with a resistance of Ri = 10^7 Ω (Figure 6). Given that EPG recordings on human hands were reported with 75 and 150 mV,[39] 50 mV was chosen a priori as a conservative starting point for recordings on mice. Recordings at 50 mV produced visible waveforms of low amplitude (Figure 6A and 6G). Increasing current to 100 mV yielded clear waveforms, so higher voltages were not investigated.

As the overall goal of this study was the safe adaptation of EPG to a mouse model in a biocontainment setting, the analysis of EPG data in the current study was limited to the published waveform library for *Ae. aegypti*[39] and a standard statistical analysis with the Ebert Generic program. Given that, to the best of our knowledge, no previous reports of AC-DC EPG recordings with live mice have been published; in-depth analysis of these data may possibly provide further insights into feeding behaviors that are not currently quantifiable.

Biosafety level 2 containment can be maintained throughout EPG reading sessions. The second aim of this study was to determine whether EPG recordings could be performed on mice using mosquitoes while maintaining a BSL-2 containment standard with enhanced BSL-3 practices. Numerous EPG studies have previously examined the effects of pathogen infection on probing and ingestion behaviors of insects that feed on plants.[9,32,34] Plant pathogens, like animal pathogens, are categorized into risk groups according to their risk and severity of infection and place of origin.[11] However, animal pathogens have special concerns associated with them because of their potential to infect the scientists performing the research as well as the vectors and hosts involved in the study. Therefore, the use of EPG to study potential animal pathogens requires the establishment of appropriate facilities and safety protocols to ensure the safety of laboratory workers. In EPG studies of plant-feeding insects, insect containment practices beyond the Faraday cage itself are typically placed outside of the Faraday cage. By placing the Faraday cage around, rather than within, the glove box, we were able to maximize the usable work area while maintaining the electrical conditions required for successful EPG recordings. Initial concerns surrounding the experimental setup included potential static electricity from the acrylic glove box and ambient electrical noise within an urban academic research building. Key aspects of the successful system were determined to be all 6 sides of the Faraday cage covered in conductive mesh or fabric panels, high electrical continuity across all these panels, and a single ground point for the ring stand holding the head stage amplifier.

Although mice were prepared in the biosafety cabinet located outside of the primary ACL-2 containment room, ABSL-2 practices were maintained when manipulating the mice. After the mice were anesthetized and prepped for EPG recordings, they were safely transferred from the biosafety cabinet into the glove box along with the small acclimation box that housed the tethered mosquitoes. The box originally chosen was too large (17″ × 7″ × 12″) and did not allow for fluid manipulation of the mosquitoes and EPG equipment while the glove box door was closed. Choosing a smaller acclimation box (8″ × 3.5″ × 5.5″) is imperative for maintaining the biosafety practices sought in this research. Future studies involving viremic mosquitoes will need to use a disinfecting and HEPA filtered vacuum pump or other mechanism to restrain mosquitoes for wiring. Such equipment is commercially available, and this limitation is unlikely to be an impediment to using this technology with viremic mosquitoes. Although the anesthesia cocktail used did not induce a long enough surgical plane of anesthesia to be ideal for EPG studies, alternative cocktails were not investigated. Other common anesthesia regimens should provide the desired 30-min sedation window, and this is unlikely to impose a limitation on future studies in this field.

Another important piece to consider when working with infectious diseases is the process for decontamination. Although the acrylic box can withstand disinfectant chemicals, proper decontamination of the EPG equipment requires special care since many of the metal components are sensitive to corrosive disinfectants such as bleach and ozone. It was determined by the Tulane Institutional Biosafety Committee that 70% ethanol would be sufficient to neutralize common enveloped viruses and not damage or corrode the components of the EPG instrument.

This work outlines procedures for performing EPG under ABSL-2 conditions and will serve as the foundation for future work to understand the effects of infection with risk group 2 pathogens on the probing and ingestion behaviors of hematophagous insects. The results from this study demonstrate the novel use of AC-DC EPG in a mouse model in ABSL-2 and ACL-2 conditions and will also serve as a blueprint for developing more advanced procedures for studying the effects of higher risk pathogens on their arthropod vectors.

Acknowledgments

We thank Dr. Anastasia Cooper for her excellent technical assistance and training with AC-DC EPG systems, Dr. Astri Wayadande for generously loaning the AC-DC EPG system used in this study, Dr. Timothy Ebert for his assistance in troubleshooting the Ebert Generic program, and Dr. Elaine Backus for her guidance on preparing the laboratory to conduct EPG studies. The following reagent was

obtained through BEI Resources, NIAID, NIH: *Aedes aegypti*, Strain ROCK, MRA-734, contributed by David W. Severson. Mention of trade names or commercial products in this publication is solely for the purpose of providing specific information and does not imply recommendation or endorsement by the U.S. Department of Agriculture. The conclusions in this report are those of the authors and do not necessarily represent the views of the USDA. USDA is an equal opportunity provider and employer.

References

1. [Internet] [Internet]. Vector-borne diseases. Available at: https://www.who.int/news-room/fact-sheets/detail/vector-borne-diseases
2. **Backus EA.** 1994. History, development, and applications of the AC electronic monitoring system for insect feeding, p. 1–51. In: Ellbury MM, Backus EA, Ullman DL**, editors.** History, development, and application of AC electronic insect feeding monitors. Lanham (MD): Entomological Society of America. https://doi.org/10.4182/UFCH1592.1994.1
3. **Backus EA, Bennett WH.** 2009. The AC-DC correlation monitor: New EPG design with flexible input resistors to detect both R and emf components for any piercing-sucking hemipteran. J Insect Physiol **55**:869–884. https://doi.org/10.1016/j.jinsphys.2009.05.007.
4. **Backus EA, Brown J.** 2016. Sharpshooter feeding behavior in relation to transmission of *Xylella fastidiosa*: A model for foregut-borne transmission mechanisms, p. 175–193. In: Brown J**,** editor. Vector-mediated transmission of plant pathogens, St. Paul (MN): APS Press. https://doi.org/10.1094/9780890545355.013
5. **Backus EA, Cervantes FA, Guedes RNC, Li AY, Wayadande AC.** 2019. AC-DC electropenetrography for in-depth studies of feeding and oviposition behaviors. Ann Entomol Soc Am **112**:236–248. https://doi.org/10.1093/aesa/saz009.
6. **Backus EA, Cline AR, Ellerseick MR, Serrano MS.** 2007. *Lugus hesperus* (Hemiptera: Miridae) feeding on cotton: New methods and parameters for analysis of nonsequential electrical penetration graph data. Ann Entomol Soc Am **100**:296–310. https://doi.org/10.1603/0013-8746(2007)100[296:LHHMFO]2.0.CO;2.
7. **Backus EA, Guedes RNC, Reif KE.** 2021. AC-DC electropenetrography: Fundamentals, controversies, and perspectives for arthropod pest management. Pest Manag Sci **77**:1132–1149. https://doi.org/10.1002/ps.6087.
8. **Backus EA, Habibi J, Yan FM, Ellersieck M.** 2005. Stylet penetration by adult *Homalodisca coagulata* on grape: Electrical penetration graph waveform characterization, tissue correlation, and possible implications for transmission of *Xylella fastidiosa*. Ann Entomol Soc Am **98**:787–813. https://doi.org/10.1603/0013-8746(2005)098[0787:SPBAHC]2.0.CO;2.
9. **Backus EA, Morgan DJW.** 2011. Spatiotemporal colonization of *Xylella fastidiosa* in its vector supports the role of egestion in the inoculation mechanism of foregut-borne plant pathogens. Phytopathology **101**:912–922. https://doi.org/10.1094/PHYTO-09-10-0231.
10. **Buitrago S, Martin TE, Tetens-Woodring J, Belicha-Villanueva A, Wilding GE.** 2008. Safety and efficacy of various combinations of injectable anesthetics in BALB/c mice. J Am Assoc Lab Anim Sci **47**:11–17.
11. **Chosewood LC, Wilson DE, Centers for Disease Control and Prevention. (U.S.), National Institutes of Health (U.S.).** 2009. Biosafety in microbiological and biomedical laboratories, 5th ed. Washington (DC): U.S. Department of Health and Human Services, Public Health Service, Centers for Disease Control and Prevention, National Institutes of Health.
12. **Choumet V, Attout T, Chartier L, Khun H, Sautereau J, Robbe-Vincent A, Brey P, Huerre M, Bain O.** 2012. Visualizing non infectious and infectious anopheles gambiae blood feedings in naive and saliva-immunized mice. PLoS One **7**:e50464. https://doi.org/10.1371/journal.pone.0050464.
13. **Ebert TA, Backus EA, Shugart HJ, Rogers ME.** 2018. Behavioral plasticity in probing by *Diaphorina citri* (Hemiptera, Liviidae): Ingestion from phloem versus xylem is influenced by leaf age and surface. J Insect Behav **31**:119–137. https://doi.org/10.1007/s10905-018-9666-0.
14. **Ebert TA, Rogers ME.** 2016. Effect of substrate voltage on EPG recordings of ingestion and probing behavior in *Diaphorina citri* (Hemiptera: Liviidae). Fla Entomol **99**:528–534. https://doi.org/10.1653/024.099.0328.
15. **Fish R, Danneman PJ, Brown M, Karas A.** 2008. Anesthesia and analgesia in laboratory animals. Academic Press.
16. **Gallup JL, Sachs JD.** 2001. The economic burden of malaria. Am J Trop Med Hyg **64** 1_suppl:85–96. https://doi.org/10.4269/ajtmh.2001.64.85.
17. **Griffiths RB, Gordon RM.** 1952. An apparatus which enables the process of feeding by mosquitoes to be observed in the tissues of a live rodent; together with an account of the ejection of saliva and its significance in malaria. Ann Trop Med Parasitol **46**:311–319. https://doi.org/10.1080/00034983.1952.11685536.
18. **Guarneri AA, Diotaiuti L, Gontijo NF, Gontijo AF, Pereira MH.** 2000. Comparison of feeding behaviour of *Triatoma infestans*, *Triatoma brasiliensis* and *Triatoma pseudomaculata* in different hosts by electronic monitoring of the cibarial pump. J Insect Physiol **46**:1121–1127. https://doi.org/10.1016/S0022-1910(99)00222-X.
19. **Guarneri AA, Diotaiuti L, Gontijo NF, Gontijo AF, Pereira MH.** 2003. Blood-feeding performance of nymphs and adults of *Triatoma brasiliensis* on human hosts. Acta Trop **87**:361–370. https://doi.org/10.1016/S0001-706X(03)00121-9.
20. **Institute of Laboratory Animal Resources (U.S.). Committee on Care and Use of Laboratory Animals.** Guide for the care and use of laboratory animals, 8th ed. Bethesda (MD): NIH Publication, U.S. Department of Health and Human Services, Public Health Service.
21. **Kashin P.** 1966. Electronic recording of the mosquito bite. J Insect Physiol **12**:281–286. https://doi.org/10.1016/0022-1910(66)90143-0.
22. **Kashin P, Wakeley HG.** 1965. An insect 'bitometer'. Nature **208**:462–464. https://doi.org/10.1038/208462a0.
23. **Kuno G.** 2010. Early history of laboratory breeding of *Aedes aegypti* (Diptera: Culicidae) focusing on the origins and use of selected strains. J Med Entomol **47**:957–971. https://doi.org/10.1603/ME10152.
24. **Levin-Arama M, Abraham L, Waner T, Harmelin A, Steinberg DM, Lahav T, Harlev M.** 2016. Subcutaneous compared with intraperitoneal ketamine–xylazine for anesthesia of mice. J Am Assoc Lab Anim Sci **55**:794–800.
25. **Lima-Camara TN, Bruno RV, Luz PM, Castro MG, Lourenco-de-Oliveira R, Sorgine MHF, Peixoto AA.** 2011. Dengue infection increases the locomotor activity of *Aedes aegypti* females. PLoS One **6**:e17690. https://doi.org/10.1371/journal.pone.0017690.
26. **Maciel-de-Freitas R, Sylvestre G, Gandini M, Koella JC.** 2013. The influence of dengue virus serotype-2 infection on *Aedes aegypti* (Diptera: Culicidae) motivation and avidity to blood feed. PLoS One **8**:e65252. https://doi.org/10.1371/journal.pone.0065252.
27. **Margalit J, Galun R, Rice M.** 1972. Mouthpart sensilla of the tsetse fly and their function: I: Feeding patterns. Ann Trop Med Parasitol **66**:525–536. https://doi.org/10.1080/00034983.1972.11686856.
28. **Platt KB, Linthicum KJ, Myint KSA, Innis BL, Lerdthusnee K, Vaughn DW.** 1997. Impact of dengue virus infection on feeding behavior of *Aedes aegypti*. Am J Trop Med Hyg **57**:119–125. https://doi.org/10.4269/ajtmh.1997.57.119.
29. **Reif KE, Backus EA.** 2021. AC–DC electropenetrography unmasks fine temporal details of feeding behaviors for two tick species on unsedated hosts. Sci Rep **11**:2040. https://doi.org/10.1038/s41598-020-80257-6.
30. **Reynolds ES, Hart CE, Hermance ME, Brining DL, Thangamani S.** 2017. An overview of animal models for arthropod-borne viruses. Comp Med **67**:232–241.
31. **Sachs J, Malaney P.** 2002. The economic and social burden of malaria. Nature **415**:680–685. https://doi.org/10.1038/415680a.
32. **Shugart H, Ebert T, Gmitter F, Rogers M.** 2019. The power of electropenetrography in enhancing our understanding of host plant-vector interactions. Insects **10**:407. https://doi.org/10.3390/insects10110407.

33. **Sim S, Ramirez JL, Dimopoulos G.** 2012. Dengue virus infection of the *Aedes aegypti* salivary gland and chemosensory apparatus induces genes that modulate infection and blood-feeding behavior. PLoS Pathog **8**:e1002631. https://doi.org/10.1371/journal.ppat.1002631.
34. **Stafford CA, Walker GP, Ullman DE.** 2011. Infection with a plant virus modifies vector feeding behavior. Proc Natl Acad Sci USA **108**:9350–9355. https://doi.org/10.1073/pnas.1100773108.
35. **Tatchell RJ, Carnell R, Kemp DH.** 1972. Electrical studies on the feeding of the cattle-tick, *Boophilus microplus*. Z Parasitenkd **38**:32–44. https://doi.org/10.1007/BF00259482.
36. **Tolle MA.** 2009. Mosquito-borne diseases. Curr Probl Pediatr Adolesc Health Care **39**:97–140. https://doi.org/10.1016/j.cppeds.2009.01.001.
37. **Walker G.** 2000. A beginner's guide to electronic monitoring of homopteran probing behavior, p. 14–40. In: Walker GP, Backus EA, editors. Principles and applications of electronic monitoring and other techniques in the study of homopteran feeding behavior, Lanham (MD): Thomas Say Publications in Entomology, Entomological Society of America.
38. **Walker GP, Backus EA.** 1992. Principles and applications of electronic monitoring and other techniques in the study of homopteran feeding behavior. Proceedings of the Symposium at the XIX International Congress of Entomology, Entomological Society of America, Beijing, China.
39. **Wayadande AC, Backus EA, Noden BH, Ebert T.** 2020. Waveforms from stylet probing of the mosquito *Aedes aegypti* (Diptera: Culicidae) measured by AC-DC electropenetrography. J Med Entomol **57**:353–368. https://doi.org/10.1093/jme/tjz188.
40. **Wei Xiang BW, Saron WAA, Stewart JC, Hain A, Walvekar V, Misse D, Thomas F, Kini RM, Roche B, Claridge-Chang A, St John AL, Pompon J.** 2022. Dengue virus infection modifies mosquito blood-feeding behavior to increase transmission to the host. Proc Natl Acad Sci USA **119**:e2117589119. https://doi.org/10.1073/pnas.2117589119.